

Field dependence of the hopping drift velocity in semiconductor superlattices

S. Rott, N. Linder, and G. H. Döhler

Institut für Technische Physik I, Universität Erlangen, Erwin-Rommel-Strasse 1, Germany

(Received 13 November 2001; published 19 April 2002)

The electronic transport in biased semiconductor superlattice structures is investigated on the basis of hopping transitions between the partially localized states of the Wannier-Stark ladder. The drift velocity is calculated numerically by summing all transitions between any two states of the ladder according to their respective weight due to the overlap of the superlattice wave functions and the microscopic scattering process. Both elastic (ionized impurity) and inelastic (acoustic and LO phonon) scattering has been taken into account. Two distinct field ranges are observed depending on the relation between the Wannier-Stark spacing eFd and the width of the lowest miniband Δ . For moderate fields ($eFd < \Delta$) the drift velocity is inversely proportional to the applied field for all scattering processes. For $eFd > \Delta$ the discrete nature of the Wannier-Stark ladder leads to a $1/F^n$ dependence of the drift velocity on the applied field, where n depends on the scattering mechanism and is larger than 1. Resonances in the drift velocity due to the discrete LO phonon energy and due to resonant tunneling into excited states are observed and discussed in detail. Simplified analytical expressions for the hopping drift velocity at low and high fields are given.

DOI: 10.1103/PhysRevB.65.195301

PACS number(s): 73.61.-r, 72.10.-d, 72.20.Ht

I. INTRODUCTION

Electronic transport perpendicular to the layers of a superlattice structure has been a field of growing interest ever since the famous starting paper of Esaki and Tsu.¹ In spite of the strongly simplifying assumptions concerning the scattering of miniband electrons in the Esaki-Tsu theory, this one-dimensional model served very well in explaining the occurrence of negative differential conductivity (NDC) along with the Bloch oscillations at high fields in these structures. The extension of this model to finite temperatures and distinct momentum and energy relaxation times² is still used by many people for fitting their experimental data.

It was, however, very soon realized that negative differential conductivity could alternatively be explained in terms of a description of transport by hopping transitions between the rungs of the Wannier-Stark (WS) ladder.^{3,4} In this model the negative differential conductivity results from the decreasing overlap of the WS states at different sites of the superlattice due to the field-induced localization of the wave functions. At that time, however, only the hopping transitions between the first and second neighboring rungs of the Stark ladder could be computed numerically. The resulting drift velocity, therefore, was only valid at sufficiently high fields F , i.e., when the spatial extent of the Wannier-Stark wave function Δ/eF (see Fig. 1) becomes smaller than two times the superlattice period d (Δ is the width of the lowest miniband).

This numerical shortcoming of the original papers on hopping transport led to the fact that in several discussions in literature on the validity of the above models⁵⁻⁷ hopping was usually ruled out as the mechanism responsible for the occurrence of NDC and it was assumed that hopping transport can only be observed in weakly coupled superlattices with very small miniband widths. For this reason most of the following theoretical investigations in this field were based on a treatment of transport in momentum space,^{2,8,9} even though it was shown that the hopping transport equation of Ref. 3

could be derived from density matrix theory by choosing the Wannier-Stark levels as basis states.^{10,11} The few papers published on hopping conduction in superlattices were of rather theoretical interest and did not provide calculations of the drift velocity for realistic superlattices.^{10,12}

Even though it was soon realized that at moderately high fields the localization effect of the Wannier-Stark wave functions is equivalent to the occurrence of Bloch oscillations in the NDC regime,^{13,14} it has been established only very recently that in the field range of Bloch oscillating electrons both the miniband and the hopping transport picture are equivalent descriptions for superlattice transport.^{15,16,20} In particular, it was shown that the criterion for the validity of the hopping picture is that the Bloch frequency $\omega_B = eFd/\hbar$ is larger than the scattering rate $1/\tau$. As this is also the condition for the onset of NDC, it was found that the hopping picture has a much broader range of applicability than was previously thought.

In this paper we closely investigate the field dependence of the hopping drift velocity for strongly coupled GaAs/AlAs superlattices. We consider both elastic (ionized impurity) and

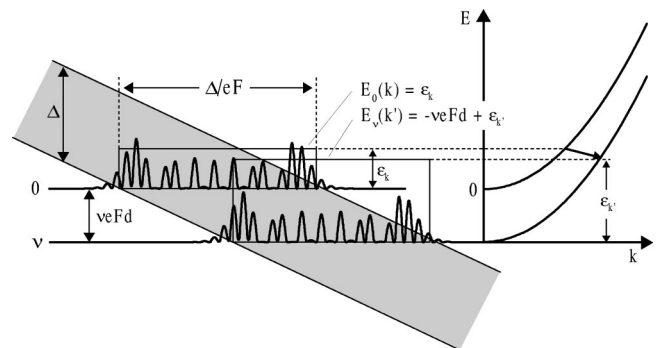


FIG. 1. Schematic diagram of an inelastic hopping transition from an initial state $|0\mathbf{k}\rangle$ with energy $E_0(\mathbf{k})$ to a final state $|\nu\mathbf{k}'\rangle$. The energy of the final state is $E_\nu(\mathbf{k}') = E_0(\mathbf{k}) \pm \hbar\omega_{\vec{q}}$, where \vec{q} is the transferred phonon momentum.

inelastic (acoustic and polar optical phonon) scattering processes and we present, for the first time, quantitative numerical calculations of the drift velocity in the NDC regime due to Wannier-Stark hopping, including all relevant transitions between any two WS levels. In contrast to the popular one-dimensional miniband model,² no fitting parameters enter into our calculations and the drift velocity is calculated using microscopic scattering between the three-dimensional states of a perfect, biased superlattice. We neglect disorder effects due to interface roughness.

The outline of the paper is as follows: In Sec. II we show the detailed theory for the numerical calculation of the hopping drift velocity for the various scattering processes. In Sec. III technical details of the numerical simulation and sample parameters are presented. The field dependence of the calculated drift velocity is discussed in detail in Sec. IV. Here, analytical models for the low- and high-field limit are derived and the influence of the WS quantization on the drift velocity is discussed. We also show that the hopping theory is capable of describing resonant tunneling into higher subbands of adjacent wells (interminiband Zener tunneling). Our results will be discussed and summarized in Sec. V.

II. THEORY OF THE HOPPING DRIFT VELOCITY

In an unbiased superlattice the electron energy spectrum consists of the eigenenergies of the superlattice Bloch functions with given wave vector $\vec{k} = (k_z, \mathbf{k})$. In growth direction a miniband with width Δ and dispersion relation $\varepsilon(k_z)$ is formed. If, however, a constant external field F is applied to the superstructure, the conduction band edge is tilted by the additional electrostatic potential eFz of the electric field. In moving one period d from one well of the superlattice to the next neighboring well, the potential thus drops by a value of eFd . Due to the large superlattice constants of several nanometers this potential drop may take values up to the order of 100 meV at high fields. Due to the invariance of the potential under the operation ($z \rightarrow z + d, E \rightarrow E - eFd$) the energy spectrum is now given by the Wannier-Stark ladder with equidistant energy states $|\nu, \mathbf{k}\rangle$, where ν denotes the WS-ladder index and \mathbf{k} is the wave vector parallel to the layers. The kinetic energy for parallel motion, ε_k , is given by a parabolic dispersion with an effective mass m_{\parallel} that is obtained by averaging the GaAs and AlAs effective masses according to the respective probability densities of the superlattice wave function in the GaAs wells and AlAs barriers.

The electronic motion in field direction in this Wannier-Stark picture is achieved through scattering processes that induce hopping transitions between the otherwise stationary WS-levels (see Fig. 1). The drift velocity is given³ by

$$v_{dr} = \sum_{\nu=1}^{\infty} \frac{v d}{\tau_{\nu}} = \sum_{\nu=1}^{\infty} v d (w_{0 \rightarrow \nu} - w_{\nu \rightarrow 0}), \quad (1)$$

where the sum is over all transitions from one state of the Wannier-Stark ladder to any state further down the ladder. Here, $1/\tau_{\nu} = w_{0 \rightarrow \nu} - w_{\nu \rightarrow 0}$ is the net hopping rate for the transition $|0\rangle \rightarrow |\nu\rangle$. The term $w_{0 \rightarrow \nu}$ is given by summing the scattering rate $S(0\mathbf{k}, \nu\mathbf{k}')$ over all initial (\mathbf{k}) and final (\mathbf{k}')

wave vectors of the 2D-electron gas belonging to the 0th and the ν th Wannier-Stark level, respectively. We obtain

$$w_{0 \rightarrow \nu} = \frac{2}{n^{(2D)}} \sum_{\mathbf{k}} \sum_{\mathbf{k}'} f(k) [1 - f(k')] S(0\mathbf{k}, \nu\mathbf{k}'). \quad (2)$$

The factor 2 accounts for the spin degeneracy of the initial \mathbf{k} states and we assume that the spin is not changed during the scattering process. The 2D density of the electron gas perpendicular to the growth direction $n^{(2D)} = n^{(3D)} d$ and the electron distribution function $f(k)$ are assumed to be independent of the Wannier-Stark level index ν due to the translational invariance of the superlattice. The scattering rate $S(0\mathbf{k}, \nu\mathbf{k}')$ depends on the scattering process and can be calculated by using Fermi's golden rule.

For an equilibrium phonon distribution,

$$S(\nu\mathbf{k}', 0\mathbf{k}) = \exp\left(\frac{E_{\nu}(k') - E_0(k)}{k_B T}\right) S(0\mathbf{k}, \nu\mathbf{k}') \quad (\text{“detailed balance”}), \quad (3)$$

and Eq. (1) can be written as

$$v_{dr} = \sum_{\nu=1}^{\infty} \nu d \frac{2}{n^{(2D)}} \sum_{\mathbf{k}} \sum_{\mathbf{k}'} S(0\mathbf{k}, \nu\mathbf{k}') f(k) [1 - f(k')] \times \left(1 - \exp\left(\frac{E_{\nu}(k') - E_0(k)}{k_B T}\right) \frac{f(k') [1 - f(k)]}{f(k) [1 - f(k')]} \right). \quad (4)$$

If field-induced heating of the electron distribution is negligible, $f(k)$ can be approximated by a Fermi distribution $(e^{\varepsilon_k/k_B T} + 1)^{-1}$ with lattice temperature. Indeed this is reasonable for lattice temperatures above about 100 K as we have shown recently.¹⁷ The term in brackets on the right-hand side of Eq. (4) then reduces to $(1 - e^{-veFd/k_B T})$ and the drift velocity thus becomes

$$v_{dr} = \sum_{\nu=1}^{\infty} \nu d w_{0 \rightarrow \nu}(F) (1 - e^{-veFd/k_B T}). \quad (5)$$

A. Phonon scattering

For simplicity, we assume that the superlattice phonon dispersion can be approximated by the bulk material modes of GaAs. By summing over all lattice modes \vec{q} the transition rate becomes

$$w_{0 \rightarrow \nu}^{ph}(F) = \frac{2}{n^{(2D)}} \frac{1}{(2\pi)^2} \int d\mathbf{k} \frac{1}{(2\pi)^2} \int d\mathbf{k}' \frac{1}{(2\pi)^3} \int d\vec{q} f(k) \times [1 - f(k')] \frac{2\pi}{\hbar} |\langle \nu\mathbf{k}', n_{\vec{q}} \pm 1 | H_{el-ph} | 0\mathbf{k}, n_{\vec{q}} \rangle|^2 \times \delta(\varepsilon_k - \varepsilon_{k'} \mp \hbar \omega_{\vec{q}} + veFd). \quad (6)$$

Here, the upper and lower signs refer to phonon emission and absorption, respectively. The electron-phonon interaction in quasi-two-dimensional semiconductor structures can be expressed as²¹

$$\begin{aligned} & |\langle \nu \mathbf{k}', n_{\bar{q}} \pm 1 | H_{el-ph} | 0 \mathbf{k}, n_{\bar{q}} \rangle|^2 \\ & = c(q) \delta_{\mathbf{k}-\mathbf{k}' \mp \mathbf{q}} (n_{\bar{q}} \pm \frac{1}{2} \pm \frac{1}{2}) |\langle \nu | e^{\mp i q_z z} | 0 \rangle|^2, \end{aligned} \quad (7)$$

where

$$\begin{aligned} c(q) &= \frac{\hbar e^2 \omega_0}{2} \left(\frac{1}{\epsilon_\infty} - \frac{1}{\epsilon} \right) \frac{q^2}{(q^2 + q_0^2)^2} \\ & \text{(polar optical phonon scattering),} \\ &= \frac{D_A^2 \hbar}{2 \rho c_s} q \quad \text{(acoustic phonon scattering).} \end{aligned} \quad (8)$$

Here, ω_0 is the optical phonon frequency, ϵ_∞ and ϵ are the high-frequency and static permittivity, q_0 is the reciprocal screening length of the 3D-electron gas, D_A is the deformation potential, ρ is the mass density, and c_s is the velocity of sound in the semiconductor material.

Inserting Eq. (7) into Eq. (6) and using the momentum-conserving δ function to eliminate the \mathbf{q} integration one obtains

$$\begin{aligned} w_{0 \rightarrow \nu}^{ph}(F) &= \frac{2}{n^{(2D)}} \frac{1}{(2\pi)^3 \hbar} \int k dk \int k' dk' \int d\theta f(k) \\ & \times [1 - f(k')] \int dq_z c(q) (n_{\bar{q}} \pm \frac{1}{2} \pm \frac{1}{2}) \\ & \times |\langle \nu | e^{\mp i q_z z} | 0 \rangle|^2 \delta(\epsilon_k - \epsilon_{k'} \mp \hbar \omega_{\bar{q}} + \nu e F d), \end{aligned} \quad (9)$$

where θ is the angle between \mathbf{k} and \mathbf{k}' , and $q = q(k, k', \theta, q_z)$ is given by

$$q = \sqrt{\mathbf{q}^2 + q_z^2}, \quad \mathbf{q}^2 = k^2 + k'^2 - 2kk' \cos \theta. \quad (10)$$

Finally, substituting $k' dk' = m_{\parallel} / \hbar^2 d\epsilon_{k'}$ and using the energy-conserving δ function, the transition rate becomes

$$\begin{aligned} w_{0 \rightarrow \nu}^{ph}(F) &= \frac{2}{n^{(2D)}} \frac{1}{(2\pi)^3} \frac{m_{\parallel}}{\hbar^3} \int k dk \int d\theta f(k) \\ & \times [1 - f(k')] \int dq_z c(q) (n_{\bar{q}} \pm \frac{1}{2} \pm \frac{1}{2}) \\ & \times |\langle \nu | e^{\mp i q_z z} | 0 \rangle|^2. \end{aligned} \quad (11)$$

Here

$$\epsilon_{k'} = \epsilon_k + \nu e F d \mp \hbar \omega_{\bar{q}} \quad \text{and} \quad k' = \frac{1}{\hbar} \sqrt{2m_{\parallel} \epsilon_{k'}}. \quad (12)$$

For polar optical phonon scattering $\omega_{\bar{q}} = \omega_0$ is a good approximation and Eqs. (10) and (12) can be easily solved for given k , θ , and q_z .

For acoustic phonon scattering, however, the system of Eqs. (10)+(12) is coupled by the condition $\omega_{\bar{q}} = c_s q$ (using a linear dispersion for the acoustic phonon branch). To obtain faster computation, in this case, the substitution $q_z = \pm \sqrt{q^2 - \mathbf{q}^2}$, $dq_z = q/q_z dq$ is performed in Eq. (9). Thus

$$\begin{aligned} w_{0 \rightarrow \nu}^{ap}(F) &= \frac{2}{n^{(2D)}} \frac{1}{(2\pi)^3 \hbar} \int k dk \int k' dk' \int d\theta f(k) \\ & \times [1 - f(k')] 2 \int dq \frac{q}{q_z} c_{ap}(q) \left(n_{\bar{q}} \pm \frac{1}{2} \pm \frac{1}{2} \right) \\ & \times |\langle \nu | e^{\mp i q_z z} | 0 \rangle|^2 \frac{1}{\hbar c_s} \delta \left(\frac{\epsilon_k - \epsilon_{k'} + \nu e F d}{\hbar c_s} \mp q \right) \\ &= \frac{2}{n^{(2D)}} \frac{2}{(2\pi)^3 \hbar^2 c_s} \int k dk \int k' dk' \int d\theta f(k) \\ & \times [1 - f(k')] \frac{q}{q_z} c_{ap}(q) \left(n_{\bar{q}} \pm \frac{1}{2} \pm \frac{1}{2} \right) \\ & \times |\langle \nu | e^{\mp i q_z z} | 0 \rangle|^2, \end{aligned} \quad (13)$$

where $c_{ap}(q)$ is the value given in Eq. (8) for acoustic phonon scattering and

$$\begin{aligned} q &= \pm \frac{\epsilon_k - \epsilon_{k'} + \nu e F d}{\hbar c_s}, \quad q_z = \sqrt{q^2 - \mathbf{q}^2}, \\ \mathbf{q}^2 &= k^2 + k'^2 - 2kk' \cos \theta. \end{aligned} \quad (14)$$

Now, for given integration variables of k , k' and θ , q , and q_z can be directly determined through Eqs. (14).

B. Impurity scattering

For ionized impurity scattering,

$$S_{ii}(\nu \mathbf{k}', 0 \mathbf{k}) = \frac{2\pi}{\hbar} \left| \sum_j \langle \nu, \mathbf{k}' | V_j | 0, \mathbf{k} \rangle \right|^2 \delta(\epsilon_k - \epsilon_{k'} + \nu e F d), \quad (15)$$

where the sum over j runs through all impurities of the superlattice. Assuming a homogeneous doping density and ensemble averaging over all impurity positions in the structure, one finds that

$$\begin{aligned} & \left\langle \left| \sum_j \langle \nu, \mathbf{k}' | V_j | 0, \mathbf{k} \rangle \right|^2 \right\rangle_{ens.av.} \\ &= \frac{N^{(2D)}}{d} \int dz_0 |\langle \nu | V_{\mathbf{k}-\mathbf{k}'}(z-z_0) | 0 \rangle|^2. \end{aligned} \quad (16)$$

$N^{(2D)}$ is the number of impurities per superlattice period. Within the three-dimensional Thomas-Fermi theory the screened impurity potential is given by

$$V_{\mathbf{q}}(z-z_0) = \frac{e^2}{2\epsilon_0} \frac{1}{|\mathbf{q}_{eff}|} e^{-|\mathbf{q}_{eff}||z-z_0|}, \quad |\mathbf{q}_{eff}| = \sqrt{\mathbf{q}^2 + q_0^2}, \quad (17)$$

where q_0 is the reciprocal Debye screening length.²²

Inserting Eqs. (15) and (16) into Eq. (2), the transition rate for impurity scattering becomes

$$w_{0 \rightarrow \nu}^{ii}(F) = \frac{2}{n^{(2D)}} \frac{1}{(2\pi)^3} \int k dk \int k' dk' \int d\theta f(k) \\ \times [1 - f(k')] \frac{2\pi}{\hbar} \frac{N^{(2D)}}{d} \int dz_0 \\ \times |\langle \nu | V_{\mathbf{k}-\mathbf{k}'}(z-z_0) | 0 \rangle|^2 \delta(\varepsilon_k - \varepsilon_{k'} + \nu eFd). \quad (18)$$

Using the δ function to perform the integration over k' , one finally obtains

$$w_{0 \rightarrow \nu}^{ii}(F) = \frac{2}{n^{(2D)}} \frac{1}{(2\pi)^2} \frac{N^{(2D)}}{d} \frac{m_{\parallel}}{\hbar^3} \int k dk \int d\theta f(k) \\ \times [1 - f(k')] \int dz_0 |\langle \nu | V_{\mathbf{k}-\mathbf{k}'}(z-z_0) | 0 \rangle|^2, \quad (19)$$

where k' is determined by energy conservation for elastic scattering

$$k' = \sqrt{k^2 + \frac{2m_{\parallel}}{\hbar^2} \nu eFd}, \quad (20)$$

and $\mathbf{q} = \mathbf{k} - \mathbf{k}'$ is given by Eq. (14).

III. NUMERICAL SIMULATION OF THE HOPPING DRIFT VELOCITY

In the following we will present results for the hopping drift velocity as a function of electric field for a sample consisting of 12 monolayers GaAs and six monolayers AlAs. The superlattice period in this structure is $d = d_{\text{Well}} + d_{\text{Barrier}} = 5.1$ nm, where $d_{\text{Well}} = 3.4$ nm and $d_{\text{Barrier}} = 1.7$ nm. The resulting width of the lowest miniband is 20.3 meV, i.e., the wells of the superlattice are strongly coupled. The minigap separation between the lowest and the first excited miniband is about 500 meV. Thus, the occupation of higher minibands is small and conduction occurs only in the lowest miniband at moderate fields where interminiband Zener tunneling may be neglected. The electron density was taken to be equal to a homogeneous doping density $N^{(3D)} = N^{(2D)}/d$ of 10^{16} cm⁻³. This gives a value of 22 nm for the screening length $1/q_0$ at 77 K. The kinetic energy for electronic motion parallel to the layers was calculated in the effective mass approximation using a value $m_{\parallel} = 0.0732m_0$, where m_0 is the free electron mass.

We have numerically calculated the hopping drift velocity at different lattice temperatures for fields ranging from 500 V/cm to 2×10^6 V/cm, corresponding to an energy spacing of the Wannier-Stark states ranging from $eFd = 0.255$ meV at 500 V/cm to $eFd = 1018$ meV at 2×10^6 V/cm. The onset of tunneling into states belonging to the second miniband

is found to occur at about $eFd = 700$ meV as will be shown later.

According to Eq. (1), the computed drift velocity is given by a sum over all transitions between a given Wannier-Stark state $|0\rangle$ and any state $|\nu\rangle$ at lower energy further down the ladder. For Wannier-Stark states that are separated by energies νeFd significantly larger than the miniband width Δ , the overlap between the wave functions approaches zero. Thus, only those transitions $|0\rangle \rightarrow |\nu\rangle$ contribute to the net drift velocity for which νeFd is smaller than Δ . For an applied field of 500 V/cm, this involves transitions between about 80 states while for only fields significantly larger than $F_{\Delta} = \Delta/ed = 4 \times 10^4$ V/cm is the transition to the nearest state ($\nu = 1$) important.

In Fig. 2 we show the calculated drift velocities for the various transitions $|0\rangle \rightarrow |\nu\rangle$ for $\nu = 1, \dots, 8$ (thin lines) and the total drift velocity resulting from the summation over all relevant ν (thick line). We observe that at high fields $F > F_{\Delta}$ the drift velocity is dominated by the $|0\rangle \rightarrow |1\rangle$ transition, corresponding to hopping between the localized wave functions in adjacent wells. Moving to lower fields, the Wannier-Stark wave functions become extended over an increasing number of quantum wells and, correspondingly, an increasing number of transitions contribute to the total drift velocity. Even though the individual contributions decrease at low fields, the total drift velocity diverges due to the summation over the increasing number of possible transitions. Thus, as was shown in Ref. 15, the hopping picture is only valid in the NDC regime, that is, down to fields for which the collisional broadening \hbar/τ of the Wannier-Stark states is smaller than the energetic WS-level spacing eFd . At lower fields, the electron coherence length due to scattering becomes smaller than the extent $\Lambda = \Delta/eF$ of the WS functions.

Hence, the electrons are scattered before the Wannier-Stark states can be coherently formed, and the WS-states do no longer represent an adequate basis for describing the transport. To make this point more clear, we refer to the correspondence between the semiclassical and the quantum mechanical picture at sufficiently low fields, which was mentioned in the introduction. In the semiclassical picture, the meaning of Λ is the amplitude of the real-space center-of-mass motion of an electron performing a Bloch oscillation. The condition $\hbar/\tau < eFd$ for the existence of the WS ladder corresponds directly to the condition $\omega_B \tau = eFd\tau/\hbar > 1$ for the existence of Bloch oscillations. The latter condition means that the path of an electron in k space has to be sufficiently long before its momentum becomes changed by a scattering event, i.e., $k(\tau) = (eF/\hbar)\tau > 1/d$. Formally, the time evolution of $\varepsilon(k'_z(t))$ during a Bloch oscillation is also reflected in the analytical expression for the WS wave functions $|0\rangle$ and $|\nu\rangle$ [see k_z integrals in Eq. (A1); assume k'_z be substituted by eFt/\hbar]. Then, the analytical expression for the WS wave functions corresponds to the unperturbed time evolution of $k_z(t)$ over the whole mini-Brillouin zone from $-\pi/d$ at the time $-T/2$ to π/d at the time $T/2$ (where $T = 2\pi/\omega_B = 2\pi\hbar/eFd$ is the Bloch oscillation period). Thus, the WS wave functions are no longer eigenstates of the su-

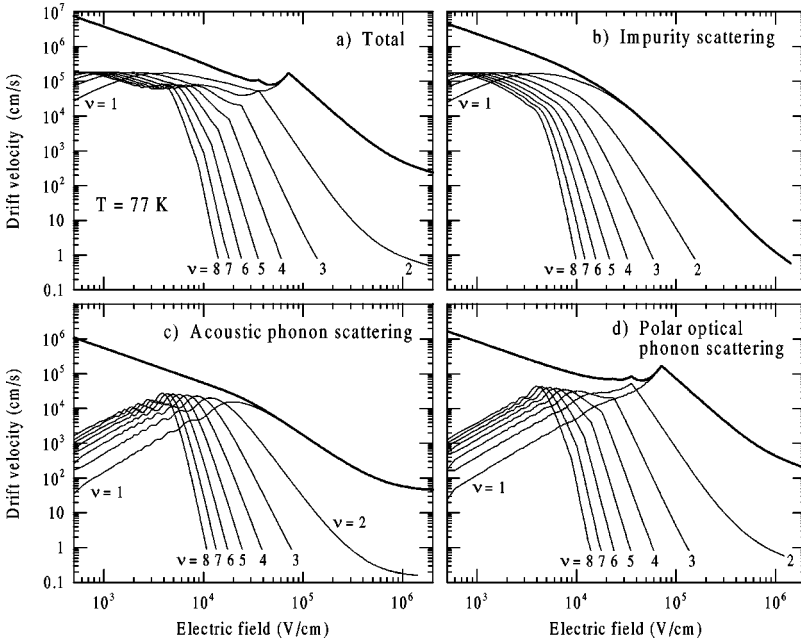


FIG. 2. Contribution of the transitions $|0\rangle \rightarrow |\nu\rangle$ (thin lines) towards the total drift velocity (thick line). The drift velocity is shown in a double logarithmic plot for the total of all scattering processes (a) and for the three single contributions (b–d).

perlattice with a uniform electric field, if $(eF/\hbar)t > 1/d$. In this case the transport has to be calculated either by following the trajectory of miniband Bloch electrons in momentum space, as achieved, for instance, by realistic Monte Carlo simulations,^{17,18} or the time evolution of miniband electrons has to be described in a formally more advanced scheme, which takes into account both hopping from quantum well to quantum well in real space and scattering processes in momentum space at an equal footing.¹⁹ The latter approach, though formally very elegant, as it is applicable and correct for the full range from very low to very high fields, unfortunately, does not allow us to take into account the scattering mechanisms in a realistic way in a reasonable numerical effort.

IV. FIELD DEPENDENCE OF THE DRIFT VELOCITY

In the following we will discuss the dependence of the drift velocity on the applied field. First we will show that at moderate fields the drift velocity obeys a $1/F$ law. This behavior corresponds to the semiclassical NDC regime of Bloch-oscillating electrons and is independent of the scattering process.

From Fig. 2 we observe, however, that significant deviations from the semiclassical $1/F$ law occur at higher fields. Here, the drift velocity is described by a power law $1/F^n$ with exponents $n > 1$, i.e., the hopping drift velocity de-

creases faster than in the semiclassical theory. The value of n depends on the scattering mechanism considered. A derivation for the values of n will be given in Sec. IV B in an analytical model that agrees very well with the numerical calculations except for very high fields.

We will also discuss the occurrence of resonances connected with the constant optical phonon energy $\hbar\omega_0$ and with the effect of resonant tunneling into excited states in neighboring quantum wells. For the latter case we go beyond the single-band approximation for the Wannier-Stark states. In both situations an increased drift velocity is observed near the resonances.

The distinct behavior for the field dependence of the drift velocity depending on the scattering process is summarized in Table I.

A. Moderate fields ($eFd < \Delta$)

To analyze the behavior of the drift velocity at moderately high electric fields, we perform a transition from the discrete Wannier-Stark states towards a quasi-energy continuum of states, corresponding to the semiclassical miniband point of view. This continuum transition may be performed if, with decreasing field F , the Wannier-Stark spacing eFd becomes much smaller than the miniband width Δ .

Starting from expression (5) the drift velocity can be rewritten in the form

TABLE I. Field dependence of the hopping drift velocity from numerical calculations. The value in brackets for impurity scattering results from the analytical model of Sec. IV B.

Field range	Acoustic phonon scattering	Polar optical phonon scattering	Impurity scattering
$eFd < \Delta$	$\propto 1/F$	$\propto 1/F$	$\propto 1/F$
$eFd > \Delta$	$\propto 1/F^2$	$\propto 1/F^3$	$\propto 1/F^{3.5(4)}$
$eFd = \hbar\omega_0/\nu$		Resonances	
$eFd = (E_1 - E_0)/\nu$	Resonant tunneling into the next highest subband		

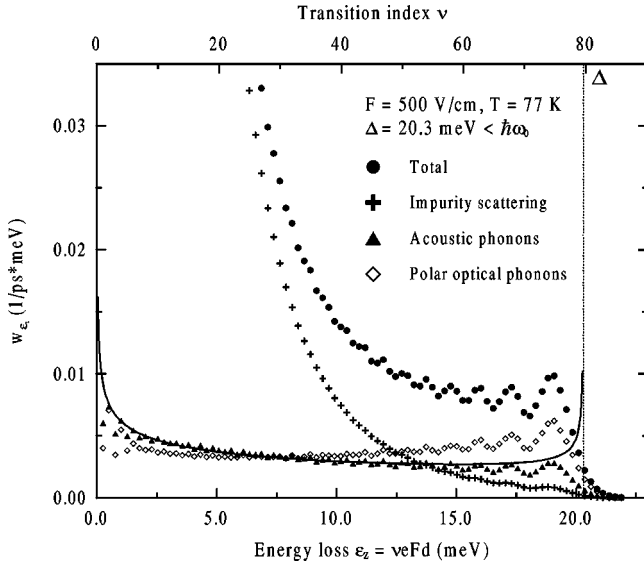


FIG. 3. The energy dependence of the transition rate $w_{\epsilon_z} = w_{0 \rightarrow \nu} / eFd$ at low fields. For the field shown, the Wannier-Stark spacing is 0.255 meV. Each point corresponds to a transition with given ν . The full line is the semiclassical result for a \mathbf{q} -independent scattering process.

$$v_{dr} = \frac{1}{eF} \sum_{\nu=1}^{\infty} \nu eFd w_{0 \rightarrow \nu}(F) (1 - e^{-\nu eFd / k_B T}). \quad (21)$$

The term νeFd corresponds to the change of energy in the electric potential associated with a hopping process that changes the center-of-mass position of the electron by the amount νd . For low fields this discrete spectrum of potential energy changes gradually turns into a quasi-continuous spectrum, characterized by the continuous energy change ϵ_z . In this case the sum over ν can be replaced by an integral over ϵ_z . Also, the discrete scattering rate $w_{0 \rightarrow \nu}$ is replaced by a scattering rate per energy $w_{\epsilon_z} = w_{0 \rightarrow \nu} / eFd$, accounting for the fact that the scattering amplitude per energy interval becomes independent of the field at low fields. The drift velocity then becomes

$$v_{dr} = \frac{1}{eF} \int_0^{\infty} d\epsilon_z \epsilon_z (1 - e^{-\epsilon_z / k_B T}) w_{\epsilon_z}, \quad (22)$$

where the integral corresponds to the semiclassical energy relaxation rate. w_{ϵ_z} is the probability per time and energy that an electron is scattered to a state for which the *potential* energy eFz in the electric field is reduced by a factor ϵ_z . It should be pointed out that the scattering-induced change of *total* energy of the electron is typically different, as it includes the change of in-plane *kinetic* energy due to scattering from \mathbf{k} to \mathbf{k}' .

We have performed numerical calculations of w_{ϵ_z} for the different scattering processes. The results for $F = 500$ V/cm are shown in Fig. 3. Our calculations show that w_{ϵ_z} is indeed independent of the electric field at low fields.

According to Eq. (22), this agrees with the fact that the resulting hopping drift velocity becomes proportional to $1/F$ at low fields.

In analyzing the energy dependence of w_{ϵ_z} , we first observe that the transition rate goes to zero for energies larger than the miniband width due to the vanishing overlap of the Wannier-Stark wave functions. The curve for impurity scattering can be qualitatively explained by the fact that the coupling constant in this case is proportional to $1/q^4$ and that with increasing energy loss ϵ_z in z -direction the transferred momentum parallel to the layers increases roughly according to $\epsilon_z \propto q^2$. For acoustic phonon scattering the coupling constant is approximately independent of ϵ_z and the small decrease of w_{ϵ_z} with energy in this case results from the decreasing overlap of the corresponding wave functions. Finally, as the miniband width Δ is smaller than $\hbar\omega_0$, only those electrons that are thermally excited parallel to the layers may undergo LO phonon emission. For the transition $|0\rangle \rightarrow |\nu\rangle$ the minimum energy for LO phonon emission is $\epsilon_k = \hbar\omega_0 - \nu eFd = \hbar\omega_0 - \epsilon_z$. Therefore, the number of electrons that may emit LO phonons and thus also the resulting scattering rate both increase slightly with increasing ϵ_z .

For the case of a \mathbf{k} independent scattering process, a link to the semiclassical, one-dimensional miniband model may now be established by approximating the scattering rate as

$$w_{\epsilon_z} = \frac{D_{comb}^{1D}(\epsilon_z)}{\tau}, \quad (23)$$

$$D_{comb}^{1D}(\epsilon_z) = \int_{\epsilon_z}^{\Delta} d\epsilon D^{1D}(\epsilon) D^{1D}(\epsilon - \epsilon_z),$$

where $D_{comb}^{1D}(\epsilon_z)$ is the one-dimensional combined density of states. In the one-dimensional (tight-binding) miniband picture the density of Bloch states entering into $D_{comb}^{1D}(\epsilon_z)$ is given by $D^{1D}(\epsilon_z) = 1/\pi \sqrt{\epsilon_z(\Delta - \epsilon_z)}$. The resulting curve for w_{ϵ_z} with a fitted value of 10 ps for τ is shown as full line in Fig. 3. We observe a very good agreement with the scattering rates for acoustic phonons in the hopping picture. The deviation of the other scattering rates from this semiclassical result is due to the momentum dependence of these scattering processes.

With the above approximation, the integration in Eq. (22) can be performed and we obtain

$$v_{dr} = \frac{1}{eF} \frac{\overline{\Delta \epsilon_z}}{\tau}, \quad (24)$$

$$\overline{\Delta \epsilon_z} = \int dk_z \int dk'_z [\epsilon(k_z) - \epsilon(k'_z)] \theta(\epsilon(k_z) - \epsilon(k'_z)) \times \left(1 - \exp\left[-\frac{\epsilon(k_z) - \epsilon(k'_z)}{k_B T} \right] \right).$$

Here, $\theta(x)$ is the Heavyside function and $\overline{\Delta \epsilon_z}$ is the mean energy loss per scattering event of Bloch oscillating electrons. Equation (24) thus has the meaning of an energy balance equation for Bloch oscillating electrons, balancing the

energy acquired from the field, eFv_{dr} , with the mean energy relaxation rate $\overline{\Delta\varepsilon_z}/\tau$. At a temperature of 77 K, a value of 6.5 meV for $\overline{\Delta\varepsilon_z}$ is obtained numerically. For $T \rightarrow \infty$, $\overline{\Delta\varepsilon_z}$ goes to zero and for $T=0$ K, $\overline{\Delta\varepsilon_z} = 4/\pi^2 \Delta \approx 8.23$ meV. We note that our values for $\overline{\Delta\varepsilon_z}$ differ slightly from the results obtained within the relaxation time approximation of the 1D-Boltzmann equation.² In particular, in that theory a value of $\Delta/2$ is obtained for $\overline{\Delta\varepsilon_z}$ at 0 K.

B. High fields ($eFd > \Delta$)

In order to establish a link to the original hopping transport paper by Tsu and Döhler,³ analytic expressions for the scattering matrix elements are derived in this section, using minor approximations for the treatment of umklapp processes. The resulting formulas provide power laws $1/F^n$ for the drift velocity in the limit of high fields. The exponents n are determined for different collision processes.

We calculate the field dependence of the matrix element $\langle \nu | V | 0 \rangle$, where $V(z) = e^{\mp iq_z z}$ [see Eq. (7)] in the case of phonon scattering and $V(z) = V_{\mathbf{q}}(z)$ [Eq. (17)] for impurity scattering, using the fact that the eigenfunction of the ν th Wannier-Stark state $|\nu\rangle$ can be expressed analytically²³ as

$$\psi_{\nu}(z) = \frac{\sqrt{d}}{2\pi} \int_{-\pi/d}^{\pi/d} dk_z u_{k_z}(z) e^{ik_z(z-\nu d)} e^{i/eF \int_0^z dk'_z [\varepsilon(k'_z) - \varepsilon_0]}. \quad (25)$$

Here, $\varepsilon(k_z)$ is the miniband dispersion relation and

$$\varepsilon_0 = \frac{d}{2\pi} \int_{-\pi/d}^{\pi/d} dk'_z \varepsilon(k'_z). \quad (26)$$

Assuming a tight-binding model for the dispersion and approximating umklapp processes to neighboring mini-Brillouin zones one can show (see Appendix) that

$$\begin{aligned} \langle \nu | V | 0 \rangle &\approx \frac{1}{2\pi} i^{\nu} \int_{-\infty}^{\infty} dq_z g(q_z) V(q_z) e^{i\nu(q_z d/2)} \\ &\times J_{\nu} \left(\frac{\Delta}{eFd} \sin \frac{q_z d}{2} \right), \end{aligned} \quad (27)$$

where J_{ν} is the Bessel function of order ν and $g(q_z)$ accounts for the fact that scattering to distant mini-Brillouin zones is reduced according to the form of the periodic superlattice function $u_{k_z}(z)$. Our approximation for $g(q_z)$ is equivalent to the approach of Tsu and Döhler for the calculation of the acoustic phonon scattering rate.³

Equation (27) is exact in the limit of vanishing q_z [i.e., $V(q_z) \propto \delta(q_z)$]. When, at high fields, q_z becomes of the order of the miniband Brillouin zone π/d , however, umklapp processes become increasingly important and Eq. (27) gives too low values for the scattering matrix element. This is shown in Fig. 4, where the hopping drift velocity resulting from the above equation for $\langle \nu | V | 0 \rangle$ is compared to the numerical calculation without approximations.

The slower decrease of the numerical result at very high fields is due to the fact that at these fields the wave functions

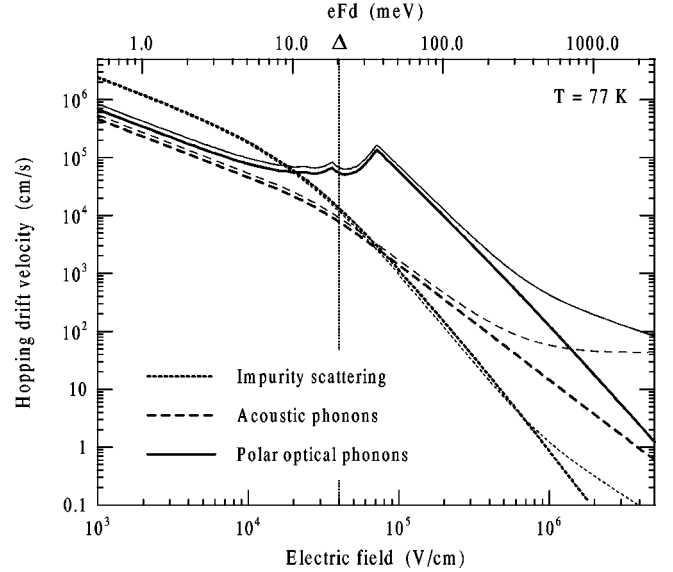


FIG. 4. Comparison of the hopping drift velocity according to Eq. (27) (thick lines) and the numerical calculation (thin lines). The two models agree very well for fields up to 4×10^5 V/cm.

[Eq. (25)] become the Wannier functions of the superlattice, which are independent of the applied field. The scattering matrix element then only contains a field dependence via the \mathbf{q} dependence of the scattering coupling constant resulting from increasing in-plane momentum transfer \mathbf{q} with increasing field. At very high fields \mathbf{q}^2 is roughly proportional to F . The scattering matrix element between the field-independent Wannier functions vanishes, however, in the approximation leading to Eq. (27).

Phonon scattering

For phonon scattering $V(q_z) = 2\pi \delta(q_z \mp q'_z)$, where q'_z is the phonon momentum in growth direction. The squared matrix element then becomes

$$\begin{aligned} &|\langle \nu | e^{\mp iq'_z z} | 0 \rangle|^2 \\ &= g(q'_z)^2 J_{\nu}^2 \left(\frac{\Delta}{eFd} \sin \frac{\pm q'_z d}{2} \right) \\ &= g(q'_z)^2 \left(\sum_{l=0}^{\infty} \frac{(-1)^l}{(\nu+l)!!} \left(\frac{\Delta}{2eFd} \sin \frac{q'_z d}{2} \right)^{\nu+2l} \right)^2. \end{aligned} \quad (28)$$

Hence the leading term in $1/F$ is of the order of $(1/F)^{2\nu}$ for the transition $0 \rightarrow \nu$.

To calculate the field dependence of the drift velocity, we now have to take into account the fact that for high fields the scattering wave vector parallel to the layers \mathbf{q} becomes approximately

$$\mathbf{q} \approx \frac{\sqrt{2m_{\parallel}(eFd \pm \hbar\omega)}}{\hbar} \propto \sqrt{F} \quad \text{for } eFd \gg \hbar\omega. \quad (29)$$

This does not introduce a field dependence into the acoustic phonon scattering rate that is independent of the value of q at sufficiently high temperatures.²⁴ For optical phonon scattering, however, a factor $1/(q_z^2 + \mathbf{q}^2)$ appears in the scattering rate. Since q_z^2 can be neglected in comparison to q^2 at high fields, this leads to an additional factor $1/F$ in the drift velocity for polar optical phonon scattering.

Hence, we find that the lowest-order term ($\nu=1$) in the reciprocal field in the high-field drift velocity is of the order $1/F^2$ for acoustic phonon scattering and of the order $1/F^3$ for polar optical phonon scattering. This is in good agreement with the slopes of the curves in Fig. 4.

Impurity scattering

By inserting Eq. (27) into Eq. (16) we obtain

$$\begin{aligned} & \frac{N}{d} \int dz_0 |\langle \nu | V_{\mathbf{k}-\mathbf{k}'}(z-z_0) | 0 \rangle|^2 \\ &= \frac{N}{4\pi^2 d} \int dz_0 \left| \int_{-\pi/d}^{\pi/d} dq_z g(q_z) V_{\mathbf{q}}(q_z) e^{i\nu(q_z d/2)} \right. \\ & \quad \left. \times J_\nu \left(\frac{\Delta}{eFd} \sin \frac{q_z d}{2} \right) e^{iq_z z_0} \right|^2 \\ &= \frac{N}{2\pi d} \int_{-\pi/d}^{\pi/d} dq_z g(q_z)^2 |V_{\mathbf{q}}(q_z)|^2 J_\nu^2 \left(\frac{\Delta}{eFd} \sin \frac{q_z d}{2} \right)^2. \end{aligned} \quad (30)$$

Here we have used the fact that the Fourier transform of $V_{\mathbf{q}}(z-z_0)$ is $e^{iq_z z_0}$ times the Fourier transform of $V_{\mathbf{q}}(z)$. Since $|V_{\mathbf{q}}(q_z)|^2$ is proportional to $1/q^4$ we expect that this q dependence of the scattering potential should add another factor $1/F^2$ to the resulting drift velocity due to impurity scattering. The total impurity-induced drift velocity should then follow a $1/F^4$ law. In Fig. 4 we observe a slope of $1/F^{3.4}$. We attribute this lower exponent to the fact that q_z cannot be completely neglected in comparison to \mathbf{q} in the integral in Eq. (30).

C. Optical phonon resonances

As the miniband width of our superlattice is smaller than the optical phonon energy $\hbar\omega_0$, normally, LO phonon emission can only occur if the electrons are heated parallel to the layers. If, however, at high fields, the spacing between any two Wannier-Stark states becomes larger than the optical phonon energy, then LO phonon emission is allowed for all electrons for the corresponding transition, and the resulting hopping rate increases considerably due to the large coupling constant for optical phonon scattering. Thus, LO phonon resonances can be observed whenever νeFd becomes equal to $\hbar\omega_0$. The resonances belonging to the individual transitions $|0\rangle \rightarrow |\nu\rangle$ can be easily recognized in Fig. 2(d).

The LO phonon resonance peaks are very pronounced at low temperatures while they become increasingly smeared out at higher temperatures due to the spreading of the electron distribution parallel to the layers. This is illustrated in

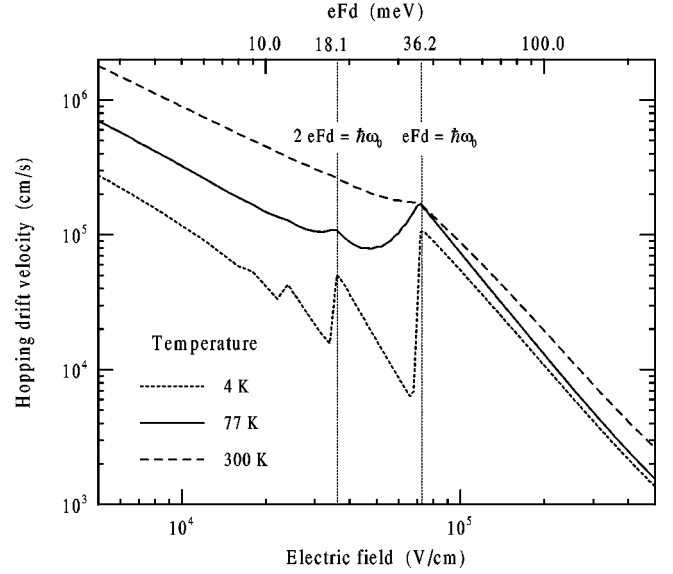


FIG. 5. The drift velocity for all scattering processes at different temperatures.

Fig. 5 that shows the total drift velocity for different temperatures. For fields eFd below $\hbar\omega_0 = 36$ meV, only hot electrons that have an energy $\epsilon_k > \hbar\omega_0 - eFd$ may undergo LO-phonon emission to the next lowest Wannier-Stark state. Therefore, the low-field slope of the resonance is determined by the electron temperature. For fields eFd larger than the optical phonon energy, polar optical phonon processes are always possible and, therefore, LO-phonon emission becomes the dominant scattering mechanism. This is also reflected by the fact that the drift velocity for fields larger than $\hbar\omega_0$ is hardly temperature dependent, since, at these temperatures, only spontaneous emission processes contribute to the drift velocity.

D. Tunneling into higher bands

At sufficiently high fields, resonant tunneling into higher states of neighboring quantum wells dominates the transport through the superlattice. In this case, the description of the electronic structure in terms of the single-band wave functions [Eq. (25)] is not valid anymore. The effect of resonant tunneling can, however, be included into our model by using the correct wave functions that have been numerically calculated for the tilted superlattice potential using the transfer matrix method with Airy functions as basis functions.²⁵ In this model we make the assumption that the tunneling times between adjacent wells are smaller than the electron lifetime due to scattering. This should be valid in our case of strongly coupled superlattices.

In our structure the resonance between the lowest subband in one well (at energy E_0) and the first subband in the adjacent well (at energy E_1) occurs at $eFd = E_1 - E_0 = \Delta_{10} \approx 700$ meV. The resulting drift velocity, including the coupling of the wave functions between neighboring wells due to resonant tunneling, is shown as dotted line in Fig. 6. Below the main resonance (at $eFd = \Delta_{10}$) two more peaks appear (at $eFd = \Delta_{10}/2$ and $eFd = \Delta_{10}/3$) due to the resonance

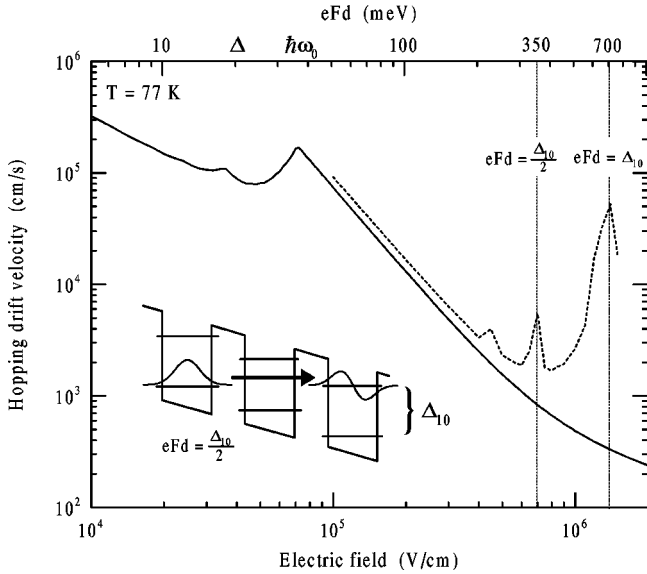


FIG. 6. The drift velocity in the single miniband approximation arising from scattering between the Kane states of Eq. (25) (full line) and with inclusion of the effect of resonant tunneling (dotted line). The inset shows the band structure and quantum well states for the field at which $2eFd = \Delta_{10}$.

of the lowest state of one well with the first excited state of the second and third next nearest well, respectively. We note that our calculation of the hopping drift velocity only includes transitions between the ground states of the (resonantly coupled) quantum wells and disregards all transitions including excited (antibonding) states of the coupled wells. For this reason and also due to the finite discretization of the applied field in the calculations shown, the height of the main resonance in Fig. 6 is quantitatively too small. Below this resonance, however, the above approximation is valid and we observe that resonant tunneling can be safely neglected for $eFd < 200$ meV, i.e., $F < 4 \times 10^5$ V/cm, in this structure.

V. DISCUSSION

We have seen that the range of electric fields in which NDC is observed can be divided in two regimes, showing different drift-velocity-field characteristics.

For moderate fields, for which eFd is smaller than Δ , the hopping velocity is characterized by a sum over several possible transitions between any two WS states separated by energies less than the miniband width. In this field regime the drift velocity obeys a $1/F$ law, independent of the microscopic scattering process. This behavior agrees with the drift velocity as given in terms of Bloch oscillating miniband electrons in a semiclassical picture. The hopping theory becomes, however, invalid in the ohmic transport regime of the semiclassical theories. The reason for this is that for low fields, for which the Bloch oscillation frequency $\omega_B = eFd/\hbar$ becomes smaller than the scattering rate $1/\tau$, the mean free path of the electron becomes smaller than the spatial extent of the WS wave function.¹⁵ At these fields the use of the WS functions as basis functions would require higher

orders of perturbation theory to describe the effect of scattering between the WS states adequately.

At high fields, characterized by $eFd > \Delta$, NDC with a different field characteristic is observed. Here, hopping is dominated by transitions between adjacent quantum wells and the drift velocity decreases with decreasing overlap of neighboring wave functions with increasing field. The drift velocity obeys a power law $1/F^n$, where n is larger than 1 and depends strongly on the microscopic scattering process. For the case of a scattering process that is independent of the transferred momentum $\mathbf{q} = \mathbf{k} - \mathbf{k}'$ a value of $n=2$ is obtained. This value has been predicted by Kazarinov and Suris for the case of nonresonant tunneling between the ground states of adjacent quantum wells²⁶ and by Döhler *et al.* for the case of acoustic phonon scattering.⁴ In this field range the spacing eFd between the nearest WS states is larger than the miniband width and the semiclassical description of transport based on the motion of Bloch electrons obviously breaks down.

Another prominent feature of the drift velocity that is due to the discrete nature of the WS ladder are the resonances due to LO phonon scattering (Fig. 5). These resonances had already been predicted in 1972 by Bryksin and Firsov²⁷ in a paper on high-field transport in ZnS. Their theory accounts for the quantum nature of the Wannier-Stark ladder by using the field- and time-dependent Houston functions²⁸ (accelerated Bloch states) instead of the Bloch states as basis in \vec{k} space. To obtain analytic results for the scattering matrix elements between the Houston states, the authors, however, had to neglect the \vec{q} dependence of LO phonon scattering. Their results are qualitatively valid but no quantitative agreement can be expected. For the case of a purely one-dimensional superlattice structure the corresponding δ -spike resonances have been described by Emin and Hart.¹²

At the position of the main LO phonon resonance an increase of the drift velocity should be observable in experiment at low temperatures. So far, however, no conclusive evidence of these resonant structures has been presented in literature. In some cases, an increase of the drift velocity at high fields may have been misinterpreted as resonant tunneling into the first excited state of the next quantum well instead of LO-phonon-induced tunneling into the ground state of the adjacent well. A clear distinction of the two different processes could be achieved by temperature-dependent measurements of the drift velocity slightly below the main resonance. Of course, it would be very instructive, if temperature-dependent domain formation between the main peak of the drift velocity at the critical field and the LO phonon resonance could be experimentally observed.

Direct measurements of the drift velocity in the NDC regime are not possible due to the formation of constant or traveling field domains. Nevertheless, there are experimental techniques that allow the determination of the drift velocity in the NDC range with good accuracy.^{29,30} Further experiments, especially with respect to the temperature dependence, would certainly provide new insights into this fascinating field.

With regard to a comparison between theory and experi-

ment a further remark, concerning the in-plane distribution function of the electrons in the Wannier-Stark levels, $f(k)$, appears to be appropriate. As mentioned in Sec. II, field-induced heating of the electrons is negligible at temperatures above about 100 K and $f(k)$ can be approximated by a Fermi distribution function with the lattice temperature. This has been found as a result of self-consistently solving the hopping rate equations for the in-plane distribution function $f(k)$.^{17,18} For temperatures below 100 K, however, strong heating is observed. Although these self-consistent distribution functions differ strongly from thermal equilibrium at larger k values, they can still be approximated by Fermi distribution functions for the (most relevant) range of smaller k values. For our 20.3-meV miniband, e.g., an electron temperature of about 100 K is obtained. As a result, the strong structure in the νdr vs field curve related to the LO phonon resonances at $\hbar\omega_0 = eFd/n$ obtained for temperatures below 77 K when the Fermi distribution of the lattice temperature is used, becomes much less pronounced and the values approach the 77-K results. For the range above 77 K the νdr vs field results are hardly affected by the self-consistent treatment of the hopping rates. A detailed discussion of the self-consistent hopping theory, however, goes beyond the scope of the present paper. It can be found in Refs. 17 and 18. It is, however, important to note that a comparison between theory and experiment for the full range down to very low temperatures has to be based on the self-consistent calculations.

ACKNOWLEDGMENTS

We would like to thank F. Köhler for providing the superlattice wave functions for our calculation of the effect of tunneling into the next miniband. S.R. acknowledges financial support by the Deutsche Forschungsgemeinschaft.

APPENDIX: CALCULATION OF THE MATRIX ELEMENT $\langle \nu | V | 0 \rangle$

Using the wave function from Eq. (25) the matrix element in z direction can be written as

$$\begin{aligned} \langle \nu | V | 0 \rangle &= \frac{d}{(2\pi)^2} \int dz V(z) \int_{-\pi/d}^{\pi/d} d\tilde{k}_z u_{\tilde{k}_z}^*(z) e^{-i\tilde{k}_z(z-\nu d)} \\ &\quad \times e^{-i/eF \int_0^{\tilde{k}_z} dk'_z [\varepsilon(k'_z) - \varepsilon_0]} \int_{-\pi/d}^{\pi/d} dk_z u_{k_z}(z) \\ &\quad \times e^{ik_z z} e^{i/eF \int_0^{\tilde{k}_z} dk'_z [\varepsilon(k'_z) - \varepsilon_0]} \end{aligned} \quad (\text{A1})$$

$$\begin{aligned} &= \frac{d}{(2\pi)^2} \int_{-\pi/d}^{\pi/d} d\tilde{k}_z \int_{-\pi/d}^{\pi/d} dk_z e^{-i\tilde{k}_z \nu d} \\ &\quad \times e^{i/eF \int_{\tilde{k}_z}^{k_z} dk'_z [\varepsilon(k'_z) - \varepsilon_0]} \int dz u_{\tilde{k}_z}^*(z) u_{k_z}(z) \\ &\quad \times e^{i(k_z - \tilde{k}_z)z} V(z). \end{aligned} \quad (\text{A2})$$

Since $u_{\tilde{k}_z}^*(z) u_{k_z}(z)$ has the periodicity of the superlattice, we can write

$$u_{\tilde{k}_z}^*(z) u_{k_z}(z) = \sum_n a_n e^{in(2\pi/d)z}, \quad (\text{A3})$$

where the a_n can be assumed to be independent of k_z and \tilde{k}_z . For the 12/6-GaAs/AlAs superlattice we obtain $a_0 = 1, a_{\pm 1} \approx 0.463$, and $a_{\pm 2} \approx -0.027$. For an investigation of the high-field dependence of the matrix element, we can expand the exponential function, giving

$$\begin{aligned} \langle \nu | V | 0 \rangle &= \frac{d}{(2\pi)^2} \sum_n a_n \int_{-\pi/d}^{\pi/d} d\tilde{k}_z \int_{-\pi/d}^{\pi/d} dk_z e^{-i\tilde{k}_z \nu d} \\ &\quad \times \sum_j \frac{1}{j!} \left(\frac{i}{eF} \int_{\tilde{k}_z}^{k_z} dk'_z [\varepsilon(k'_z) - \varepsilon_0] \right)^j \\ &\quad \times \int dz \exp \left[i \left(k_z - \tilde{k}_z + n \frac{2\pi}{d} \right) z \right] V(z). \end{aligned} \quad (\text{A4})$$

The $j=0$ term in the expansion corresponds to the ‘‘Wannier-limit,’’ that describes the reduction of the Kane functions [Eq. (25)] to Wannier functions in the high-field limit.

Assuming a tight-binding model for the dispersion relation, we can perform the k'_z integration, obtaining

$$\begin{aligned} \langle \nu | V | 0 \rangle &= \frac{d}{(2\pi)^2} \sum_n a_n \sum_j \frac{1}{j!} \left(\frac{\Delta}{4} \right)^j \frac{1}{(eFd)^j} \int_{-\pi/d}^{\pi/d} d\tilde{k}_z \\ &\quad \times \int_{-\pi/d}^{\pi/d} dk_z e^{-i\tilde{k}_z \nu d} (e^{i(k_z - \tilde{k}_z)d} - 1)^j \\ &\quad \times (e^{i\tilde{k}_z d} + e^{-i\tilde{k}_z d})^j V_q \left(k_z - \tilde{k}_z + n \frac{2\pi}{d} \right), \end{aligned} \quad (\text{A5})$$

and substituting $q_z = k_z - \tilde{k}_z + n(2\pi/d)$ we can write the above expression as

$$\begin{aligned} \langle \nu | V | 0 \rangle &= \frac{d}{(2\pi)^2} \sum_j \frac{1}{j!} \left(\frac{\Delta}{4} \right)^j \frac{1}{(eFd)^j} \int_{-\pi/d}^{\pi/d} d\tilde{k}_z e^{-i\tilde{k}_z \nu d} \\ &\quad \times \sum_n a_n \int_{-(\pi/d) - \tilde{k}_z + n(2\pi/d)}^{(\pi/d) - \tilde{k}_z + n(2\pi/d)} dq_z (e^{iq_z d} - 1)^j \\ &\quad \times (e^{i\tilde{k}_z d} + e^{-i(\tilde{k}_z + q_z)d})^j V(q_z). \end{aligned} \quad (\text{A6})$$

We now approximate the sum over n together with the integral over q_z according to

$$\sum_n a_n \int_{-(\pi/d) - \tilde{k}_z + n(2\pi/d)}^{(\pi/d) - \tilde{k}_z + n(2\pi/d)} dq_z \rightarrow \int_{-\infty}^{\infty} dq_z g(q_z), \quad (\text{A7})$$

where

$$g(q_z) = \sum_n a_n P_n(q_z), \quad (\text{A8})$$

and

$$P_n(q_z) = \frac{d}{2\pi} \int_{-\pi/d}^{\pi/d} d\tilde{k}_z \theta\left(\frac{\pi}{d} - \tilde{k}_z - q_z + n\frac{2\pi}{d}\right) \times \theta\left(\tilde{k}_z + q_z - n\frac{2\pi}{d} + \frac{\pi}{d}\right) \quad (\text{A9})$$

is the over \tilde{k}_z averaged probability that $\tilde{k}_z + q_z$ lies within the n th Brillouin zone. This approach is a generalization of the method used by Tsu and Döhler³ for the simplified calculation of the acoustic phonon hopping matrix elements.

We can thus write the scattering matrix element as

$$\langle \nu | V | 0 \rangle = \frac{d}{(2\pi)^2} \sum_j \frac{1}{j!} \left(\frac{\Delta}{4eFd}\right)^j \int_{-\infty}^{\infty} dq_z g(q_z) (e^{iq_z d} - 1)^j V(q_z) \int_{-\pi/d}^{\pi/d} d\tilde{k}_z e^{-i\tilde{k}_z \nu d} (e^{i\tilde{k}_z d} + e^{-i(\tilde{k}_z + q_z)d})^j. \quad (\text{A10})$$

When expanding the term in brackets according to

$$(e^{i\tilde{k}_z d} + e^{-i(\tilde{k}_z + q_z)d})^j = \sum_{m=0}^j \binom{j}{m} e^{i(2m-j)\tilde{k}_z d} e^{-i(j-m)q_z d} \quad (\text{A11})$$

and performing the integration in \tilde{k}_z we then obtain a sum over δ functions $\delta_{\nu, 2m-j}$ with $0 \leq m \leq j$. Using these δ functions we find that for $\nu \leq j$ and $\nu + j$ even we have

$$\langle \nu | V | 0 \rangle = \frac{1}{2\pi} \sum_{j \geq \nu} \frac{1}{j!} \left(\frac{\Delta}{4eFd}\right)^j \binom{j}{\nu+j} \int_{-\infty}^{\infty} dq_z g(q_z) V(q_z) \times (e^{iq_z d} - 1)^j \exp\left[-\frac{i}{2}(j-\nu)q_z d\right] \quad (\text{A12})$$

with the matrix element vanishing otherwise. Finally, by using $l = (j - \nu)/2$ as new summation index and applying the definition of the Bessel functions in terms of an infinite sum, we find that

$$\begin{aligned} \langle \nu | V | 0 \rangle &= \frac{1}{2\pi} \int_{-\infty}^{\infty} dq_z g(q_z) V(q_z) \sum_{l=0}^{\infty} \frac{1}{(\nu+2l)!} \left(\frac{\Delta}{4eFd}\right)^{\nu+2l} \\ &\quad \times (e^{iq_z d} - 1)^{\nu+2l} \binom{\nu+2l}{\nu+l} e^{-ilq_z d} \\ &= \frac{1}{2\pi} i^\nu \int_{-\infty}^{\infty} dq_z g(q_z) V(q_z) e^{i\nu q_z d/2} \\ &\quad \times \sum_{l=0}^{\infty} \frac{(-1)^l}{(\nu+l)! l!} \left(\frac{\Delta}{2eFd} \sin \frac{q_z d}{2}\right)^{\nu+2l} \\ &= \frac{1}{2\pi} i^\nu \int_{-\infty}^{\infty} dq_z g(q_z) V(q_z) e^{i\nu(q_z d/2)} J_\nu\left(\frac{\Delta}{eFd} \sin \frac{q_z d}{2}\right). \end{aligned} \quad (\text{A13})$$

¹L. Esaki and R. Tsu, IBM J. Res. Dev. **14**, 61 (1970).

²A. A. Ignatov, E. P. Dodin, and V. I. Shashkin, Mod. Phys. Lett. B **5**, 1087 (1991).

³R. Tsu and G. H. Döhler, Phys. Rev. B **12**, 680 (1975).

⁴G. H. Döhler, R. Tsu, and L. Esaki, Solid State Commun. **17**, 317 (1975).

⁵A. Sibille, J. F. Palmier, H. Wang, and F. Mollot, Phys. Rev. Lett. **64**, 52 (1990).

⁶X. L. Lei, N. J. M. Horing, and H. L. Cui, Phys. Rev. Lett. **66**, 3277 (1991).

⁷R. Tsu and L. Esaki, Phys. Rev. B **43**, 5204 (1991).

⁸A. A. Ignatov and V. I. Shashkin, Phys. Lett. **94A**, 169 (1983).

⁹R. R. Gerhardt, Phys. Rev. B **48**, 9178 (1993).

¹⁰D. Calecki, J. F. Palmier, and A. Chomette, J. Phys. C **17**, 5017 (1984).

¹¹R. A. Suris and B. S. Shchamkhalova, Fiz. Tekh. Poluprovodn. **18**, 1178 (1984) [Sov. Phys. Semicond. **18**, 738 (1984)].

¹²D. Emin and C. F. Hart, Phys. Rev. B **36**, 2530 (1987).

¹³F. Beltram, F. Capasso, D. L. Sivco, A. L. Hutchinson, S. G. Chu, and A. Y. Cho, Phys. Rev. Lett. **64**, 3167 (1990).

¹⁴A. Sibille, J. F. Palmier, and F. Mollot, Appl. Phys. Lett. **60**, 457 (1992).

¹⁵S. Rott, N. Linder, and G. H. Döhler, Superlattices Microstruct. **21**, 569 (1997).

¹⁶A. Wacker and A.-P. Jauho, Phys. Rev. Lett. **80**, 369 (1998).

¹⁷S. Rott, P. Binder, N. Linder, and G. H. Döhler, in *Proceedings of the 24th International Conference, on the Physics of Semiconductors, Jerusalem, 1998*, edited by D. Gershoni (World Scientific, Singapore, 1999), file 0718.

¹⁸S. Rott, in *Theory of Electronic Transport in Semiconductor Superlattices*, edited by T. Marek, S. Malzer, and P. Kiesel (Erlangen, 1999), ISBN 3-932392-16-7.

¹⁹A. Wacker, A.-P. Jauho, S. Rott, A. Markus, P. Binder, and G. H. Döhler, Phys. Rev. Lett. **83**, 836 (1999).

²⁰S. Rott, P. Binder, N. Linder, and G. H. Döhler, Phys. Rev. B **59**, 7334 (1999).

²¹B. K. Ridley, J. Phys. C **15**, 5899 (1982).

²²S. Rott, K. Schrüfer, C. Metzner, S. Müller, T. Schmidt, and G. H. Döhler, Superlattices Microstruct. **23**, 315 (1998).

²³E. O. Kane, J. Phys. Chem. Solids **12**, 181 (1959).

²⁴The factor q in $c(q)$ in Eq. (8) is compensated for by the phonon occupation number n_q in Eq. (9) which is proportional to $k_B T / \hbar c_s q$ for acoustic phonon scattering at not too low temperatures.

²⁵F. Köhler, B. Knüpfer, and N. Linder, G. Philipp, and G. H. Döhler (unpublished).

²⁶R. F. Kazarinov and R. A. Suris, Fiz. Tekh. Poluprov. **6**, 148 (1972) [Sov. Phys. Semicond. **6**, 120 (1972)].

²⁷V. V. Bryksin and Y. A. Firsov, Solid State Commun. **10**, 471 (1972). For a more modern version of this theory applied to

- superlattice transport see V. V. Bryksin and P. Kleinert, *J. Phys.: Condens. Matter* **9**, 7403 (1997).
- ²⁸W. V. Houston, *Phys. Rev.* **57**, 184 (1940).
- ²⁹E. Schomburg *et al.*, in *Proceedings of the International Conference on the Physics of Semiconductors, Berlin, 1996*, edited by M. Scheffler and R. Zimmermann (World Scientific, Singapore, 1996), p. 1679.
- ³⁰C. Rauch, G. Strasser, K. Unterrainer, W. Boxleitner, E. Gornik, and A. Wacker, *Phys. Rev. Lett.* **81**, 3495 (1998).